Stem Cell Reports
Article

ISSCR

OPEN ACCESS

PI3Kβ-regulated β-catenin mediates EZH2 removal from promoters controlling primed human ESC stemness and primitive streak gene expression

Sudhanshu Yadav,[1] Antonio Garrido,[1] M. Carmen Hernández,[1] Juan C. Oliveros,[2] Vicente Pérez-García,[3] Mario F. Fraga,[4] and Ana C. Carrera[1,5,*]

[1]Department of Immunology and Oncology, Universidad Autónoma de Madrid, Cantoblanco, 28049 Madrid, Spain
[2]Department of Systems Biology, Bioinformatics, Centro Nacional de Biotecnología/CSIC, Universidad Autónoma de Madrid, Cantoblanco, 28049 Madrid, Spain
[3]Centro de Investigación Príncipe Felipe, Eduardo Primo Yúfera, 46013 Valencia, Spain
[4]Nanomaterials and Nanotechnology Research Center/CSIC, Health Research Institute of Asturias (ISPA), Institute of Oncology of Asturias (IUOPA), Research Center for Rare Diseases (CIBERER), 33011 Oviedo, Asturias, Spain
[5]Lead contact
*Correspondence: acarrera@cnb.csic.es
https://doi.org/10.1016/j.stemcr.2022.09.003

SUMMARY

The mechanism governing the transition of human embryonic stem cells (hESCs) toward differentiated cells is only partially understood. To explore this transition, the activity and expression of the ubiquitous phosphatidylinositol 3-kinase (PI3Kα and PI3Kβ) were modulated in primed hESCs. The study reports a pathway that dismantles the restraint imposed by the EZH2 polycomb repressor on an essential stemness gene, *NODAL*, and on transcription factors required to trigger primitive streak formation. The primitive streak is the site where gastrulation begins to give rise to the three embryonic cell layers from which all human tissues derive. The pathway involves a PI3Kβ non-catalytic action that controls nuclear/active RAC1 levels, activation of JNK (Jun N-terminal kinase) and nuclear β-catenin accumulation. β-Catenin deposition at promoters triggers release of the EZH2 repressor, permitting stemness maintenance (through control of NODAL) and correct differentiation by allowing primitive streak master gene expression. PI3Kβ epigenetic control of EZH2/β-catenin might be modulated to direct stem cell differentiation.

INTRODUCTION

Human embryonic stem cells (hESCs) derive from the inner cell mass of blastocysts and possess the capacities of self-renewal and pluripotency, processes collectively known as stemness (Niwa, 2007). Understanding the mechanisms governing pluripotency, division, and differentiation is central to regeneration medicine. *OCT4* (*Octamer-Binding Protein*), *SOX2* (SRY-Box Transcription Factor 2), and *NANOG* (Homeobox Protein NANOG) are the "core" regulators of pluripotency. Although the mechanism behind stemness control in mouse ESCs has been described extensively, much less is known about the regulatory networks governing self-renewal in hESCs (Zheng et al., 2012).

To maintain stemness, hESCs need to be cultured in medium containing several growth factors (GF): basic fibroblast growth factor (bFGF), NODAL (or Activin A, both transforming growth factor β [TGF-β] family members), and insulin (INS) (or INS growth factor) (Dakhore et al., 2018). FGF triggers extracellular signal-regulated kinase (ERK) activation, which has to be restricted by phosphatidylinositol 3-kinase (PI3K) to remain at low levels and maintain stemness (high phospho (p)-ERK levels promote hESC differentiation) (Na et al., 2010; Singh et al., 2012). bFGF and INS also activate PI3K, which is also required for stemness in part because of its capacity to restrict ERK. ERK and PI3K induce *NANOG* expression (Storm et al., 2007; Yu et al., 2011). The third medium component, NODAL, triggers SMAD2 and SMAD3 transcription factor (TF) activation, which amplify *NODAL* levels via a positive feedback loop (Bertero et al., 2015). NODAL also induces *NANOG* expression (Beattie et al., 2005). As *NANOG* upregulates *OCT4* and *SOX2* (Li, 2010), bFGF, INS, and NODAL are sufficient to control the core regulators of pluripotency.

Loss of stemness is induced via intrinsic and environmental signals that push ESCs to follow their "intrinsic" differentiation pathways (Mateus et al., 2009). A critical step in mammalian embryo development is formation of the three embryonic cell layers from which the different tissues evolve (Wang et al., 2012). The ectoderm, the outermost cell layer, emerges from the epiblast at the blastula stage. Later, an invagination known as the primitive streak (PS) forms in the posterior medial region of the otherwise symmetrical blastocyst. Formation of the PS involves an epithelial-mesenchymal transition of some of the epiblast cells, which enables them to migrate toward the inner part of the embryo. Within the PS, which marks the site where gastrulation will occur, the mesoderm and endoderm cell layers begin to form. PS formation requires a set of master TFs, including *GSC*, *SOX17*, *MIXL1*, etc. PS formation is also influenced by environmental factors; e.g., NODAL and WNT (wingless/integrated) (Yoney et al.,

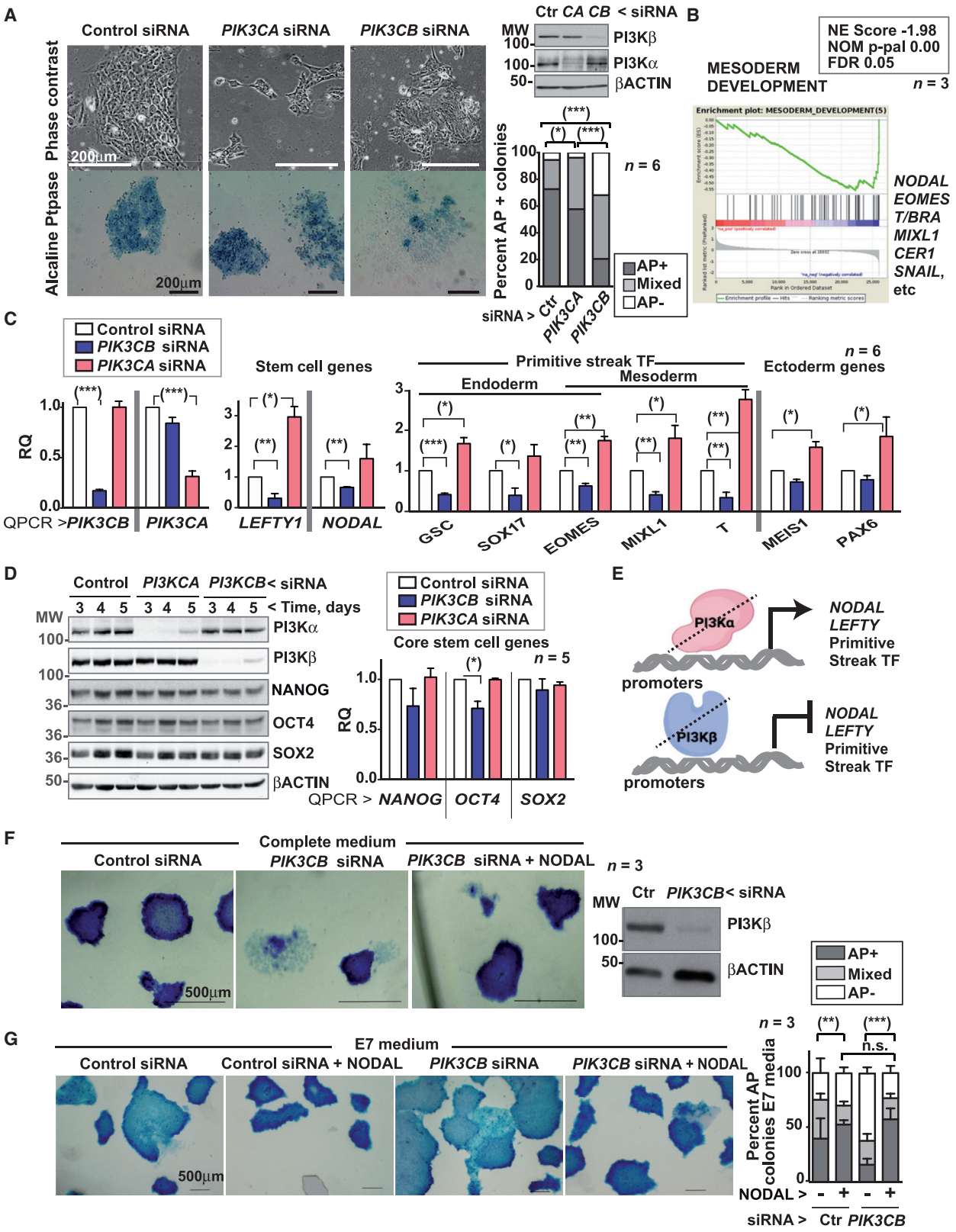

(legend on next page)

2018; Scialdone et al., 2016; Funa et al., 2015). At the PS, WNT secretion in the epiblast induces a pathway that protects β-catenin from GSK3β-mediated phosphorylation and degradation, resulting in activation of β-catenin-dependent gene expression (MacDonald and He, 2012). GSK3β inactivation (inducing β-catenin accumulation) is also triggered by PI3K and ERK (Cross et al., 1995; Ding et al., 2005). As polycomb repressive complexes (PRCs) are deposited in the promoters of differentiation genes to avoid their expression during stemness, hESC differentiation requires PRC release from these promoters (Collinson et al., 2016; Aranda et al., 2015).

As mentioned above, PI3K regulates stemness; two isoforms of PI3K are expressed in ESCs: PI3Kα and PI3Kβ. Deletion of PI3Kβ induces earlier mouse embryo death (approximately embryonic day 3 [E3]) than PI3Kα deletion (∼E9.5) (Bi et al., 1999, 2002). Mice expressing kinase-dead PI3Kβ survive to adulthood, supporting a PI3Kβ-kinase independent action in embryonic development (Ciraolo et al., 2008). Here, modulation of PI3Kα and PI3Kβ levels and activities were used to challenge hESC homeostasis and learn about stemness/differentiation decision-making. The results show that the two isoforms contribute differently to the stemness/differentiation transition. PI3Kα acts mainly as a lipid kinase and restricts ERK activity, and PI3Kβ acts as a scaffold to regulate nuclear (active) RAC1 levels, JNK activation, and β-catenin nuclear entry. We show that β-catenin triggers release of the polycombrepressor protein EZH2 (Enhancer Of Zeste 2 Polycomb Repressive Complex 2) from gene promoters, illustrating a mechanism for PRC release from the promoters of PS TFs (essential for PS formation) and of *NODAL* (essential for stemness and PS formation). The present findings offer a mechanism for displacement of PRCs from promoters at the onset of differentiation, point to involvement of β-catenin in hESC stemness maintenance, and highlight new targets for directing tissue generation.

RESULTS

PI3Kβ expression is needed for hESC pluripotency

To learn about the signaling requirements of hESCs at the stemness/differentiation transition, the action of PI3Kα and PI3Kβ was compared in hESCs. Genome-integrating methods that introduce reprogramming factors (such as viral vectors) were avoided; rather, we transiently depleted the PI3K isoforms using small interfering RNA (siRNA). Alkaline phosphatase (AP) activity, a sign of stemness, was reduced by PI3Kα depletion and more markedly by PI3Kβ depletion (Figure 1A).

Comparison gene expression analysis between PI3Kα- and PI3Kβ-depleted hESCs (72 h) (Table S1; GEO: GSE202163) showed them to be only weakly correlated (Figure S1A). More than half of the genes altered by each isoform were not altered by the other (Figure S1B). A set of genes with key functions in development (*NODAL*, *GSC*, etc.) was regulated in opposing manners by PI3Kα and PI3Kβ (Figure S1A). One of the PI3Kβ targets was *MYC* (myelocytomatosis oncogene product); because this gene controls stemness (Takahashi and Yamanaka, 2006), gene expression changes in *N*- and *C-MYC*-silenced cells was also analyzed (Table S1). More than 70% of MYC-controlled genes were unaffected by PI3Kα or PI3Kβ depletion (Figure S1B). Gene Ontology (GO) analysis showed that PI3Kβ-activated genes are related to development; MYC also regulated developmental genes, but these genes were not targets of PI3Kβ (Figure S1C; Table S1; GEO: GSE202163).

Among the genes selectively activated by PI3Kβ was a collection of TFs essential for PS formation (*GSC*, *SOX17*, *EOMES*, *MIXL1*, and *T* [*TBXT* or *Brachyury*]) and *NODAL*, a stemness-essential gene that is also required at the PS (James et al., 2005). PI3Kα and MYC exerted opposing actions than PI3Kβ on these genes (Figure S1D). Gene set enrichment analysis (GSEA) indicated PI3Kβ depletion to impair the expression of genes involved in mesoderm,

Figure 1. PI3Kβ regulates stemness by controlling *NODAL* expression

(A) Representative phase-contrast and alkaline phosphatase (AP)-stained images of hESCs transfected with *PIK3CB*, *PIK3CA*, or control siRNA (96 h). Right: western blot (WB) illustrating silencing efficiency. The graph shows the percentages of AP+, AP−, and mixed colonies; n = 6 (>50 colonies scored in each). *p < 0.05, ***p < 0.001 (chi-square test).

(B) GSEA of genes upregulated by PI3Kβ.

(C) hESCs transfected with siRNA (72 h) (n = 3) were used to prepare mRNA and cDNA. The graphs show the mRNA levels of different genes represented as RQ (relative quantification; 2-ΔΔCT) versus *GAPDH* (indicated).

(D) Core stem cell gene levels after PI3K depletion (as in C), examined with WB or quantitative real-time (qRT)-PCR.

(E) Diagram of gene expression changes after PI3Kα or PI3Kβ depletion.

(F) Representative images of AP-stained control or *PIK3CB*-silenced hESCs (96 h) grown in mTeSR1 alone or with NODAL (last 72 h, daily replacement). The WB shows silencing efficiency.

(G) AP images (as in F) of hESCs grown in mTeSR-E7 (NODAL free) with or without external added NODAL (200 ng/mL, last 72 h); graph as in (A). *p < 0.05, **p < 0.01, ***p < 0.001, t test. Original blots for all figures can be found at https://doi.org/10.17632/m9g4fcvrm8.1.

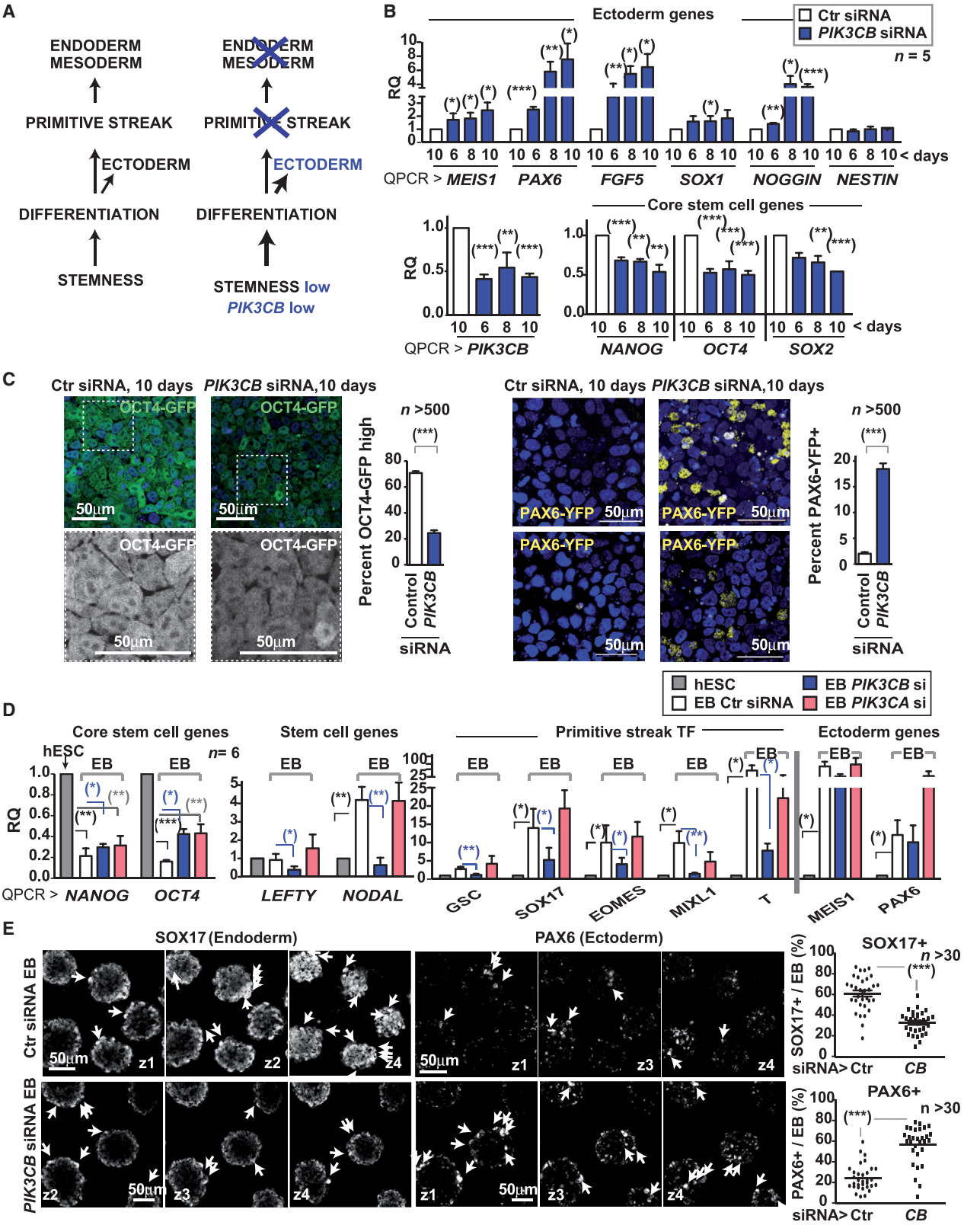

(legend on next page)

endoderm, and primary germ layer formation (Figures 1B and S1E), confirming PI3Kβ control of PS gene expression.

PI3Kβ regulates stemness by controlling NODAL expression

PI3Kβ control of *NODAL* and PS TF levels was confirmed by quantitative real-time PCR. PI3Kβ depletion reduced *NODAL* expression, that of its effector *LEFTY1*, and that of the PS TF genes *GSC*, *SOX17*, *EOMES*, *MIXL1*, and *T* without affecting the ectoderm genes *MEIS1* and *PAX6* (Figure 1C). In contrast, PI3Kα depletion increased these genes' levels as well as of *MEIS1* and *PAX6* (Figure 1C). Because NODAL is essential for pluripotency (James et al., 2005), and PI3Kβ depletion (at 72 h) caused a significant reduction in *NODAL* levels prior to reducing the core stem cell genes (mainly *OCT4*), *NODAL* seemed to be a primary target of PI3Kβ in regulation of stemness (Figures 1C and 1D). PI3Kβ controls other hESC genes (*CRABP2*, *RBPMS*, etc.) and early differentiation genes (Skottman et al., 2005; Mansergh et al., 2009; Figure S2). Thus, PI3Kβ depletion reduced (and PI3Kα increased) *NODAL* and PS TF levels (Figure 1E).

It was postulated that PI3Kβ regulates stemness by controlling *NODAL* expression. NODAL addition restored the AP signal in most PI3Kβ-depleted cells (Figure 1F). Also, hESC culture in NODAL-free medium (mTeSRE7) reduced the AP signal, which was corrected by NODAL addition (Figure 1G). PI3Kβ-depleted hESCs in mTeSRE7 exhibited an even lower AP signal, but addition of NODAL restored the AP signal (Figure 1G). This suggests that at least part of the action of PI3Kβ in stemness control relies on NODAL.

PI3Kβ regulates expression of PS genes at the onset of differentiation

Attention was next paid to the TFs that regulate PS formation. The anterior cells of murine epiblasts (E6–E6.5) give rise to ectoderm; the posterior region forms the PS where endoderm and mesoderm appear. Because PI3Kβ is required for PS TF expression, it was thought that PI3Kβ-depleted hESCs might only differentiate into ectoderm (Figure 2A). Although 72-h PI3Kβ depletion did not markedly alter stem cell markers or ectoderm genes (Figures 1C and 1D), 6 days of depletion reduced the stem cell gene levels and increased the levels of most ectoderm genes (Figure 2B).

Stemness loss and acquisition of ectoderm markers after PI3Kβ depletion was confirmed in H1 hESCs. *OCT4*-GFP (green fluorescence protein) H1 cells express GFP under control of the *OCT4* promoter, whereas PAX6-YFP (yellow fluorescence protein) H1 cells express YFP under the control of the *PAX6* promoter (Zwaka and Thomson, 2003; Yao et al., 2017). PI3Kβ depletion reduced the *OCT4*-controlled GFP signal and enhanced the *PAX6*-regulated YFP signal (Figure 2C).

In other tests, hESCs transfected with *PIK3CB* or *PIK3CA* siRNA (48 h) were cultured for 5 days to form embryoid bodies (EBs). *NANOG* and *OCT4* levels fell in control EBs but less so in PI3Kα- or β-depleted EBs; *NODAL* levels increased in control and PI3Kα-depleted EBs but not in PI3Kβ-depleted EBs (Figure 2D). Suboptimal downregulation of *OCT4* might be secondary to NODAL level defects (Sakaki-Yumoto et al., 2013). PS TF levels were reduced in PI3Kβ-depleted EBs, whereas ectoderm genes were expressed normally (Figure 2D).

The contribution of PI3Kβ to PS (endoderm and mesoderm) formation was confirmed when PI3Kβ-depleted hESCs (48 h) were placed in endoderm or mesoderm differentiation medium (5 days). Expression of the *GSC* and *SOX17* endoderm genes and of the *MIXL1* and *T* mesoderm genes required PI3Kβ expression (Figure S3A). Fluorescence analysis of day 10 EBs derived from *PAX6*-YFP H1 hESCs revealed PI3Kβ depletion to lead to an increase in the proportion of PAX6+ ectoderm cells and a reduction in that of SOX17+ endoderm cells (Figure 2E). Thus, PI3Kβ expression is required for expression of the PS TF and, in turn, for endoderm and mesoderm gene expression but not for expression of ectoderm genes.

A PI3Kβ scaffolding function regulates gene expression

To test whether the action of PI3Kβ on gene expression required its kinase activity, the consequences of inhibiting PI3Kα or PI3Kβ in hESCs were examined using

Figure 2. PI3Kβ regulates expression of PS TFs

(A) Ontogeny of the primary germ layers and effect of PI3Kβ depletion.

(B) Relative mRNA levels in hESCs after PI3Kβ depletion (for 6, 8, or 10 days).

(C) *OCT4*-GFP H1 hESCs were transfected with siRNA and examined live by microscopy. Representative images show the reduction in the *OCT4*-regulated EGFP signal in PI3Kβ-depleted hESCs. Right: representative images of the *PAX6* promoter-regulated YFP signal in control and *PIK3CB*-silenced cells. Graphs show the percentage of positive cells.

(D) Quantitative real-time PCR mRNA levels for the indicated genes in embryoid bodies (EBs). hESCs transfected with siRNA (48 h) were disaggregated and placed in EB formation medium for 72 h prior to analysis.

(E) Representative individual z sections of YFP-PAX6 and SOX17 immunofluorescence staining in control and *PIK3CB*-silenced YFP-PAX6 H1 hESCs (as in C). Arrows indicate positive cells in different sections. Graphs as in (C).

(B–E) *p < 0.05, **p < 0.01, ***p < 0.001 (t test).

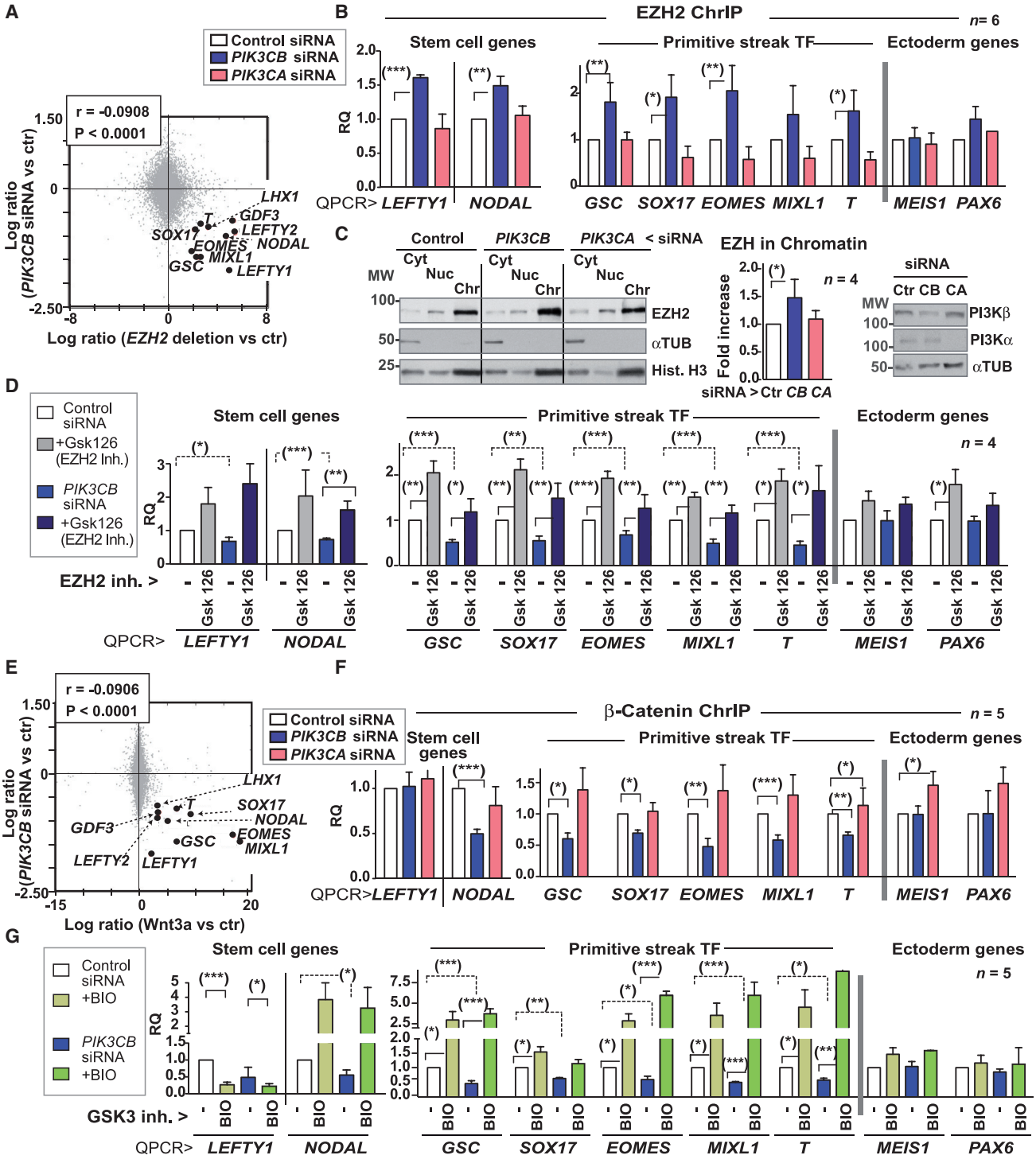

Figure 3. PI3Kβ controls EZH2 promoter occupancy and β-catenin deposition

(A) Log ratio of the mean gene expression values in EZH2-depleted hESCs versus control (x axis) (GEO: GSE76626; Collinson et al., 2016) or in PI3Kβ-depleted versus control hESCs (y axis) (GEO: GSE202163). R, Pearson's coefficient, p values.

(B) hESCs were transfected with siRNA (72 h), and EZH2 was immunoprecipitated from extracts. Shown are relative quantitative real-time PCR levels of each mRNA in complex with the ChIP versus that in whole chromatin.

(legend continued on next page)

isoform-selective inhibitors (PIK75 and TGX221) (Marqués et al., 2009). These inhibitors reduced the levels of phoshorylated (p) active form of AKT (Ak strain transforming) in control cells (Figure S3B), but, in contrast to PI3Kβ depletion, TGX221-PI3Kβ inhibition (48 h) increased *NODAL* and PS TF mRNA levels, similar to PI3Kα inhibition (Figure S3C). Accordingly, prolonged treatment with the PI3Kβ inhibitor (TGX221) did not increase ectoderm gene levels and tended to enhance PS TF expression, similar to PI3Kα inhibition or depletion (Figure S3D). These findings suggest that *NODAL* and PS TF expression relies on a PI3Kβ non-catalytic function as PI3Kβ inhibition exert a different effect. Most likely, PI3Kβ associates a macromolecule acting as a scaffold, affecting the latter's localization, stability, or activity.

PI3Kβ controls occupancy of the *NODAL* and PS TF gene promoters by EZH2

PI3Kα activity has been reported to be involved in differentiation repression (Madsen et al., 2019), but the function for PI3Kβ in hESCs is unknown. To gain insight into the action of PI3Kβ in hESCs, its gene expression signature was compared with that resulting from interference with key regulators of stemness/differentiation. Polycomb complexes ensure repression of differentiation genes during stemness. EZH2, the PRC2 catalytic component, triggers Histone3K27me3 formation, which recruits PRC1 complexes to chromatin to induce Histone2K119 ubiquitination and repression of gene expression (Aranda et al., 2015). A comparison of the genes regulated by EZH2 (Collinson et al., 2016) and by PI3Kβ revealed *NODAL*, *LEFTY1*, and the PS TF to be regulated by both (Figure 3A); approximately 25% of the genes activated by PI3Kβ were repressed by EZH2 (Figure S4A). The control exerted by PI3Kβ on EZH2 promoter occupation was tested by EZH2 chromatin immunoprecipitation (ChIP). PI3Kβ depletion (but not of PI3Kα) increased the EZH2 content at *NODAL*, *LEFTY1*, and PS TF gene promoters (but not at ectoderm gene promoters) and increased overall chromatin-bound EZH2 (Figures 3B and 3C). H2AK119Ub ChIP confirmed PI3Kβ control of PRC occupancy at *NODAL*, *LEFTY1*, and PS TF genes promoters (Figure S4B). H2AK119Ub content at *MEIS1* and *PAX6* promoters was regulated by PI3Kα and PI3Kβ (Figure S4B), an action possibly regulated by PI3K activity.

Because PI3Kβ controls EZH2 displacement from promoters, EZH2 inhibition should rescue the levels of these genes. Addition of the Gsk126 EZH2 inhibitor to PI3Kβ-depleted cells rescued *LEFTY1*, *NODAL*, and PS TF levels and did not affect *MEIS1* and *PAX6* (Figure 3D). This suggests that PI3Kβ controls *NODAL* and *PS TF* by displacing EZH2 from their promoters.

PI3Kβ regulates β-Catenin promoter deposition, and in turn EZH2 displacement

The PI3Kβ gene expression signature also resembled that induced by WNT/β-catenin (Huggins et al., 2017). *LEFTY1*, *NODAL*, and the PS TF were upregulated by WNT and PI3Kβ (Figure 3E). β-Catenin ChIP showed that PI3Kβ depletion reduced the presence of β-catenin at the *NODAL* and PS TF promoters but not at ectoderm gene promoters (Figure 3F). To confirm the requirement of PI3Kβ for β-catenin binding to the *NODAL* and PS promoters, β-catenin was activated by addition of the GSK3 inhibitor 6-bromoindirubin-3′-oxime (BIO; 24 h). BIO rescued *NODAL* and PS levels in PI3Kβ-depleted cells (Figure 3G) without affecting ectoderm genes or *LEFTY1* (a target of NODAL that might require NODAL addition; see below; Bertero et al., 2015).

Because PI3Kβ triggered EZH2 removal and β-catenin deposition at the *NODAL* and PS TF promoters, it may be that β-catenin deposition triggers release of EZH2 from these promoters. Expression of the PS TF and of *NODAL* was regulated by WNT3/β-catenin and by EZH2 (Figure 4A; datasets from Huggins et al., 2017; Collinson et al., 2016). To test β-catenin's involvement in EZH2 removal from these promoters, EZH2 ChIP was performed in cells treated with BIO, an exogenous activator of β-catenin. BIO reduced EZH2 binding to the *NODAL* and PS TF promoters in

(C) WB analysis of cytosol (Cyt), nuclear (Nuc), and chromatin (Chr) fractions from control, PI3Kβ-, or PI3Kα-depleted hESCs (72 h). Blots show depletion efficiency and fraction controls. The EZH2 signal in Chr was normalized to that of histones; the graph shows the fold increase of EZH2 bound to Chr in PI3K-depleted hESCs versus controls.

(D) Quantitative real-time PCR mRNA levels in control or *PIK3CB*-silenced cells (72 h) treated or not treated with the EZH2 inhibitor (Gsk126, 5 μM, last 24 h).

(E) Log ratio of the mean gene expression values in WNT3a-treated hESCs (24 h) versus controls (GEO: GSE103175; Huggins et al., 2017) and of PI3Kβ-depleted hESCs versus controls, as in (A).

(F) Binding of β-catenin to promoters, as determined by ChIP as in (B). hESCs were transfected with the indicated siRNA (72 h); ChIP was performed using an anti-β-catenin antibody (Ab).

(G) hESCs were transfected with siRNA (72 h) and treated with the GSK3 inhibitor 6-bromoindirubin-3′-oxime (BIO; 2 μM) for the last 24 h. The graphs show the RNA levels.

(B–D, F, and G) Mean ± SD, $n \geq 4$; *$p < 0.05$, **$p < 0.01$, ***$p < 0.001$ (unpaired t test).

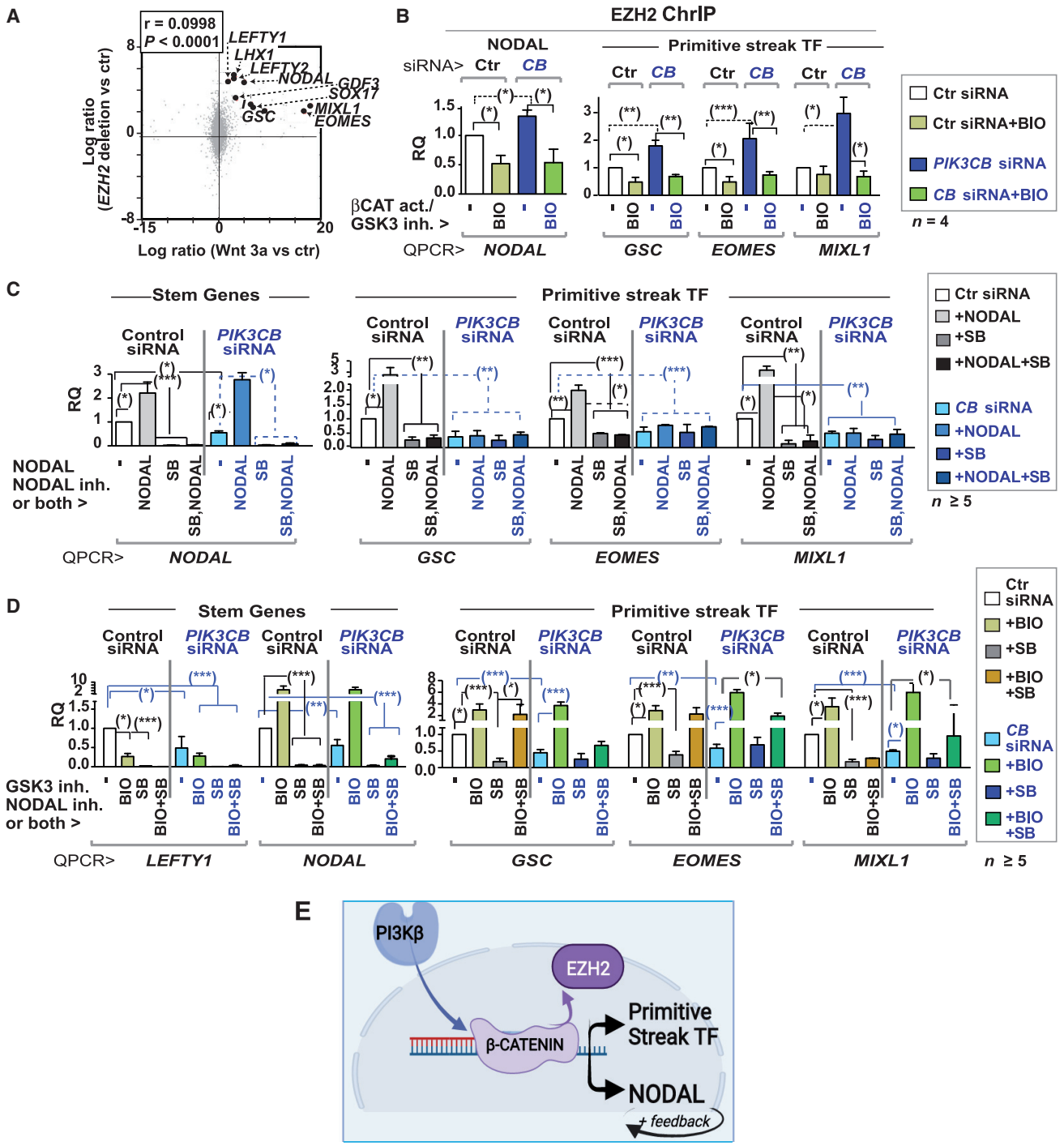

Figure 4. PI3Kβ regulated β-catenin-induced EZH2 promoter displacement, and JNK activation rescues Nuc β-catenin and gene expression in PI3Kβ-depleted hESCs

(A) WNT3a (GEO: GSE103175; Huggins et al., 2017) versus EZH2 (GEO: GSE76626; Collinson et al., 2016) gene expression patterns.

(B) ChIP testing of EZH2 promoter occupancy in control and *PIK3CB*-silenced cells (72 h) incubated with or without BIO (2 μm) for the last 48 h.

(C) mRNA levels in control or PI3Kβ-depleted cells after culture in mTeSR1 alone (72 h), with NODAL (100 ng/mL, last 24 h), with SB (a NODAL inhibitor, 10 μm, 24 h), or with both.

(legend continued on next page)

control hESCs (Figure 4B), showing that β-catenin triggers EZH2 release in intact hESCs. BIO also corrected the EZH2 excess at *NODAL* and PS TF promoters in PI3Kβ-depleted cells (Figure 4B).

One of the genes regulated by EZH2/β-catenin exchange is *NODAL,* which itself regulates PS gene expression (Greber et al., 2008). The relative contribution of NODAL to PS gene expression was examined. NODAL addition increased *NODAL* levels in controls and in PI3Kβ-depleted cells (Figure 4C) (because *NODAL* is regulated by positive feedback), and this effect was blocked by the SB431542NODAL/TGFβ inhibitor. NODAL also increased PS gene expression in control cells but did not rescue PS gene expression upon PI3Kβ depletion (Figure 4C). Therefore, the defect in PS TF expression in PI3Kβ-depleted cells is not secondary to NODAL reduced levels.

In contrast, *NODAL* and PS TF mRNA levels were rescued by exogenous activation of β-catenin (using BIO) in PI3Kβ-depleted cells (Figure 4D). *NODAL* expression still required NODAL-derived signals (it was reduced by SB431542 [SB]) but activation of β-catenin rescued PS TF levels in control and PI3Kβ-depleted cells (and PS TFs levels were only partially reduced by SB) (Figure 4D). Thus, NODAL helps, but β-catenin makes an essential contribution to PS TF expression.

β-Catenin activation requires the inputs of PI3K activity and PI3Kβ expression

To examine the mechanism behind the distinct actions of PI3Kα and PI3Kβ in hESCs, first we compared the levels of both isoforms in hESCs and EBs (using Jurkat cells for normalization) (Marqués et al., 2009). PI3Kβ was more abundant in hESCs, and both isoform levels decreased in EBs (Figure S4C). To tests the consequences of short-time PI3Kα or PI3Kβ inhibition, hESCs were incubated in GF-free medium and then exposed to PI3Kα or PI3Kβ inhibitors (1 h) in the presence of INS or bFGF (for the last 20 min). PI3Kα and PI3Kβ inhibition reduced PI3K pathway activation (pAKT, pp70S6K, and pGSK3β) and increased pERK levels (Figure S4D), as in hESCs treated with a pan-PI3K inhibitor (Singh et al., 2012). Despite pERK levels showing a slightly greater dependence on PI3Kβ (with bFGF) and on PI3Kα (with INS) (Figure S4D), this difference did not explain the opposing actions of PI3Kα or PI3Kβ depletion on gene expression (Figure 1C).

Because the amount of nuclear active β-catenin (ABC) and of β-catenin was very low at 20 min of INS and bFGF treatment (data not shown), activation time was increased to 1–2 h, when INS and bFGF increased cytosolic pAKT and nuclear ABC/β-catenin levels (Figure S5A). The fluctuations of pAKT levels with INS treatment have been reported previously (Olazábal-Morán et al., 2021).

Because PI3Kα and PI3Kβ inhibition induced similar effects on the PI3K pathway and ERK (see above), additional PI3K effectors were considered. We examined p-Ser552-β-catenin levels (regulated by AKT), which modulate β-catenin nuclear entry (Fang et al., 2007). p-Ser552-β-catenin levels paralleled those of pAKT without explaining the need of PI3Kβ for nuclear β-catenin accumulation (data not shown). Active forms of RAC1 and RAP1 enter the nucleus and have been linked to β-catenin nuclear entry (Wu et al., 2008; Griffin et al., 2018). These GTPases are generally activated at the plasma membrane (PM) and migrate to the nucleus in its active form (discussed below). INS and bFGF increased nuclear RAP1 and RAC1 in parallel to the augmentation of nuclear β-catenin levels (Figure S5A).

To examine the consequences of short-term PI3K inhibition on nuclear β-catenin levels, hESCs were activated with INS (1 h) in the presence of a PI3Kβ (TGX221) or pan-PI3K (Ly294002) inhibitor. Both inhibitors reduced pAKT levels and nuclear RAP1, RAC1, and ABC/β-catenin levels (Figure 5A). A similar assay compared PI3Kβ depletion (72 h) and PI3Kβ inhibition (90 min). Short-time PI3Kβ inhibition (but not PI3Kβ depletion) reduced pAKT levels (Figure 5B). Although nuclear RAP1 was similarly affected by PI3Kβ inhibition and depletion, PI3Kβ depletion more markedly reduced nuclear RAC1 and β-catenin levels, (Figure 5B). This pointed to RAC1, but not RAP1, as a potential target of PI3Kβ.

Because the consequences of depleting PI3Kα versus PI3Kβ on gene expression were tested at 72 h and those of inhibiting PI3Kα or PI3Kβ at 48 h (Figures 1 and S3), these conditions were used to examine PI3Kβ control of nuclear β-catenin levels. Despite depletion (72 h) and prolonged inhibition (48 h) of PI3Kα or PI3Kβ increased pERK (as it is restricted by PI3K), these treatments failed to reduce AKT activation and instead increased pAKT levels (Figure 5C). This is due to the mechanism cells have to ensure transient PI3K pathway activation, which, after induction, triggers a negative feedback mechanism that reduces its activity (Rozengurt et al., 2014). Prolonged PI3K inhibition eliminates the negative feedback that restrains PI3K/PDK1 and results in AKT/PI3K pathway upregulation (see below; scheme in Figure S6B). Because PI3K depletion and prolonged PI3K inhibition increased pAKT levels (Figure 5C), the AKT/PI3K pathway cannot be considered

(D) RNA transcript levels in control and PI3Kβ-depleted hESCs after 72 h incubation in mTeSR1 alone, with BIO (2 μm), with SB (10 μm), or with both (indicated) for the last 24 h.
(B–D) Mean ± SD *p < 0.05, **p < 0.01, ***p < 0.001 (t test).
(E) Model showing that PI3Kβ-modulated β-catenin deposition at *NODAL* and PS TF promoters triggers EZH2 displacement.

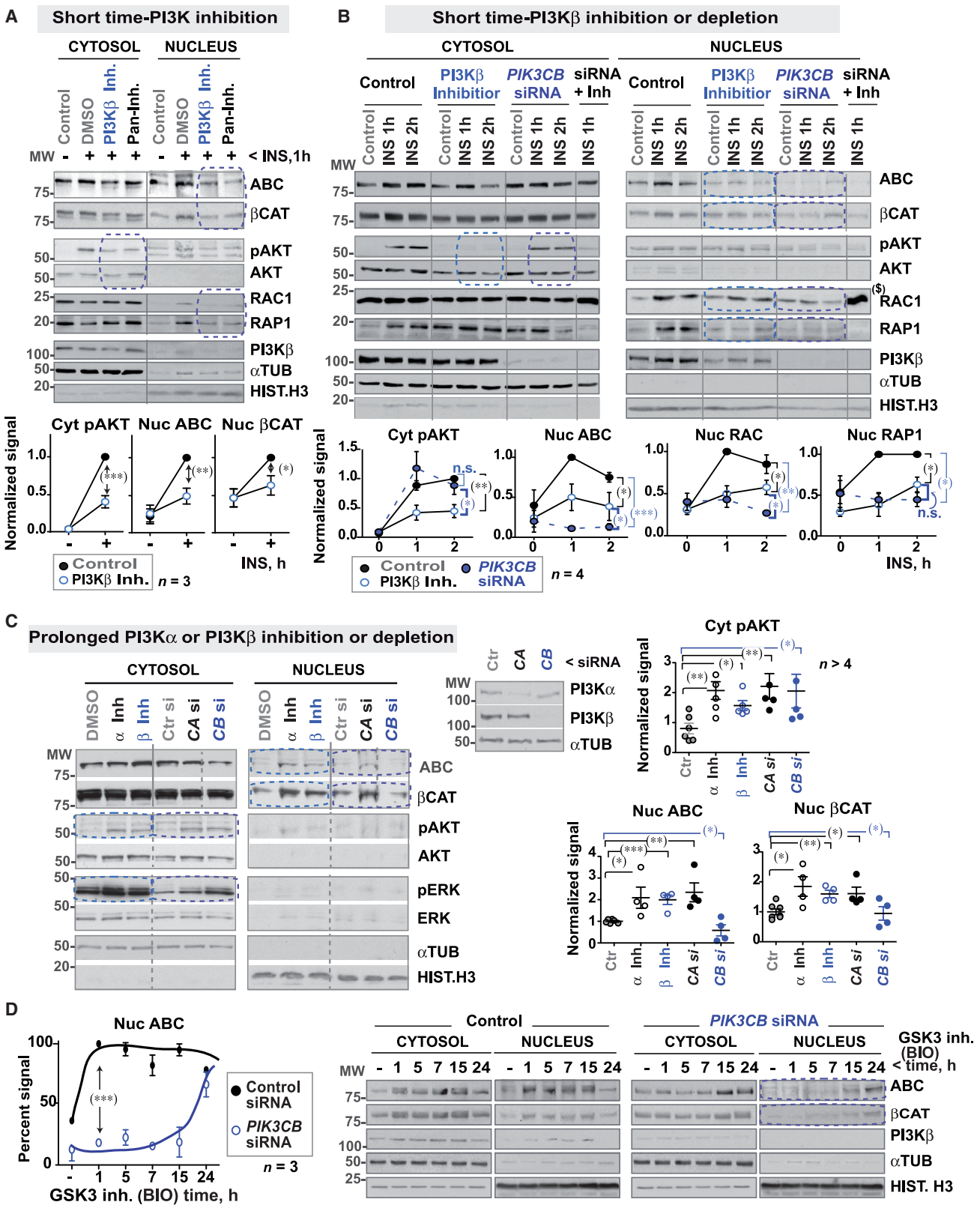

(legend on next page)

inhibited under these treatments. A common effect of short-term and long-term PI3K inhibition (or depletion) is an increase in ERK activity, which reduces hESC stemness (Na et al., 2010). Thus, the action of PI3Kα depletion or prolonged inhibition on gene expression could be a consequence of the increased ERK and AKT activities. PI3Kβ depletion also increased pAKT and pERK but showed a dominant effect at reducing β-catenin nuclear levels (Figure 5C).

Activation of β-catenin using the GSK3 inhibitor BIO (24 h) rescued gene expression in PI3Kβ-depleted cells (Figure 3); PI3Kβ regulation of nuclear β-catenin was tested upon BIO treatment. PI3Kβ depletion reduced β-catenin nuclear levels up to 15 h after BIO addition; after 24 h, BIO compensated for the PI3Kβ requirement for nuclear β-catenin accumulation (Figure 5D). Thus, PI3Kβ also controls nuclear β-catenin levels induced by GSK3 inhibitors.

PI3Kβ controls nuclear β-Catenin by regulating the RAC1 and JNK axis

Reconstitution experiments were needed to confirm the kinase-independent function of PI3Kβ in β-catenin nuclear accumulation. Because transfection was of very low efficiency and high toxicity in hESCs, reconstitution assays were performed in HEK293T cells. Treatment of these cells with distinct stimuli (1 h or 4 h) increased nuclear β-catenin levels (Figure S5B). In HEK293T cells treated with INS, PI3Kα depletion (72 h) did not significantly affect pAKT levels but increased pERK and nuclear β-catenin levels (Figure S5C). PI3Kβ depletion (72 h) did not affect pAKT or pERK levels but, as in hESCs, it markedly reduced β-catenin nuclear levels (Figure S5C). To confirm the kinase-independent action of PI3Kβ on nuclear β-catenin, HEK293T cells were PI3Kβ depleted (72 h) and then reconstituted by transfection of wild-type (WT) or inactive (K>R-805) PI3Kβ (for the last 48 h); extracts were resolved in three fractions. PI3Kβ depletion reduced, and WT or K>R-805 (KR) PI3Kβ rescued, nuclear β-catenin levels; RAC1 nuclear levels paralleled those of β-catenin (Figure 6A). This confirmed the kinase-independent PI3Kβ effect on nuclear β-catenin accumulation and the parallel revovery by reconstituted PI3Kβ of nuclear-active β-catenin and RAC.

RAC1 activates JNK; JNK phosphorylates β-catenin and increases its nuclear entry in WNT-activated ST2 cells (Wu et al., 2008). In HEK293T cells, INS increased cytosolic phospho (p)JNK levels (independent of PI3Kβ) and PM pJNK levels in a PI3Kβ-dependent manner (Figure 6A). Because RAC1 and JNK are often activated at the PM (Han et al., 1998; Neisch et al., 2010), we confirmed that GFs also induced translocation of PI3Kβ to the PM (Figure S5D).

Despite the fact that the exact mechanism of PI3Kβ regulation of active RAC1 nuclear levels requires further study, the parallel control by PI3Kβ of PM pJNK levels and of PM/nuclear active RAC1 levels (Figure 6A) suggests that RAC1 activation at the PM might promote JNK activation at this site. JNK activation at the PM would trigger β-catenin nuclear translocation. This hypothesis was tested in HECK293T cells. First, V^{12}RAC1 was transfected in HEK293T cells; this did not rescue nuclear β-catenin levels in PI3Kβ-depleted cells, but V^{12}RAC1 expression levels were very low in PI3Kβ-depleted cells compared with controls (data not shown), supporting PI3Kβ control of active RAC1 levels. Second, if the mechanism of PI3Kβ action involves the RAC1/JNK axis, then exogenous activation of JNK (using anisomycin or sorbitol) should rescue nuclear β-catenin levels in PI3Kβ-depleted cells. The two JNK activators increased PM pJNK levels and corrected nuclear β-catenin levels in PI3Kβ-depleted cells (Figure S6A), suggesting that PI3Kβ controls nuclear β-catenin in a RAC1/JNK-dependent manner.

To confirm that this route was acting in hESCs, JNK activation was rescued with sorbitol (anisomycin gave similar results). Sorbitol equalized PM pJNK levels in control and PI3Kβ-depleted hESCs and corrected nuclear β-catenin in PI3Kβ-depleted cells (Figure 6B). A similar assay was used

Figure 5. hESCs growth in mTeSR1, INS treatment, and GSK3 inhibition trigger PI3Kβ-dependent β-catenin Nuc localization

(A) hESCs were pre-incubated in GF-free medium (16 h); incubated with DMSO, TGX221 (30 μM), or LY294002 (10 μM) for 90 min; and then treated with INS (10 μg/mL) (last 60 min). Extracts were examined in WB. Graphs show the signals corrected with the loading control and normalized to the signal at 1 h (INS).

(B) hESCs were transfected with control or *PIK3CB* siRNA (72 h) or incubated with TGX221 (30 μM, 30 min) prior to INS addition (10 μg/mL) (1 or 2 h). The $ symbol in RAC1 blots indicates that the signal corresponds to the 25-kDa molecular weight (MW) marker (in this lane). Bots and graphs are as in (A).

(C) hESCs grown on mTeSR1 were transfected with siRNA (72 h) or incubated with PI3Kα or PI3Kβ inhibitors (0.1 μM PIK75 or 30 μM TGX221) (48 h). Extracts were examined by WB. Dashed vertical lines indicate sliced lanes. Graphs are as in (A). Signals were normalized to the signal in controls.

(D) WB analysis of the fractions from control or PI3Kβ-depleted hESCs (96 h) incubated in GF-free medium (last 24 h) with BIO (2 μm; added for the indicated times). The graph shows the ABC signal corrected for loading and relative to the signal in 1-h BIO-treated controls.

(A–D) Mean ± SD, $n \geq 3$; *$p < 0.05$, **$p < 0.01$, ***$p < 0.001$ (t test). Ellipses call attention to the most relevant data.

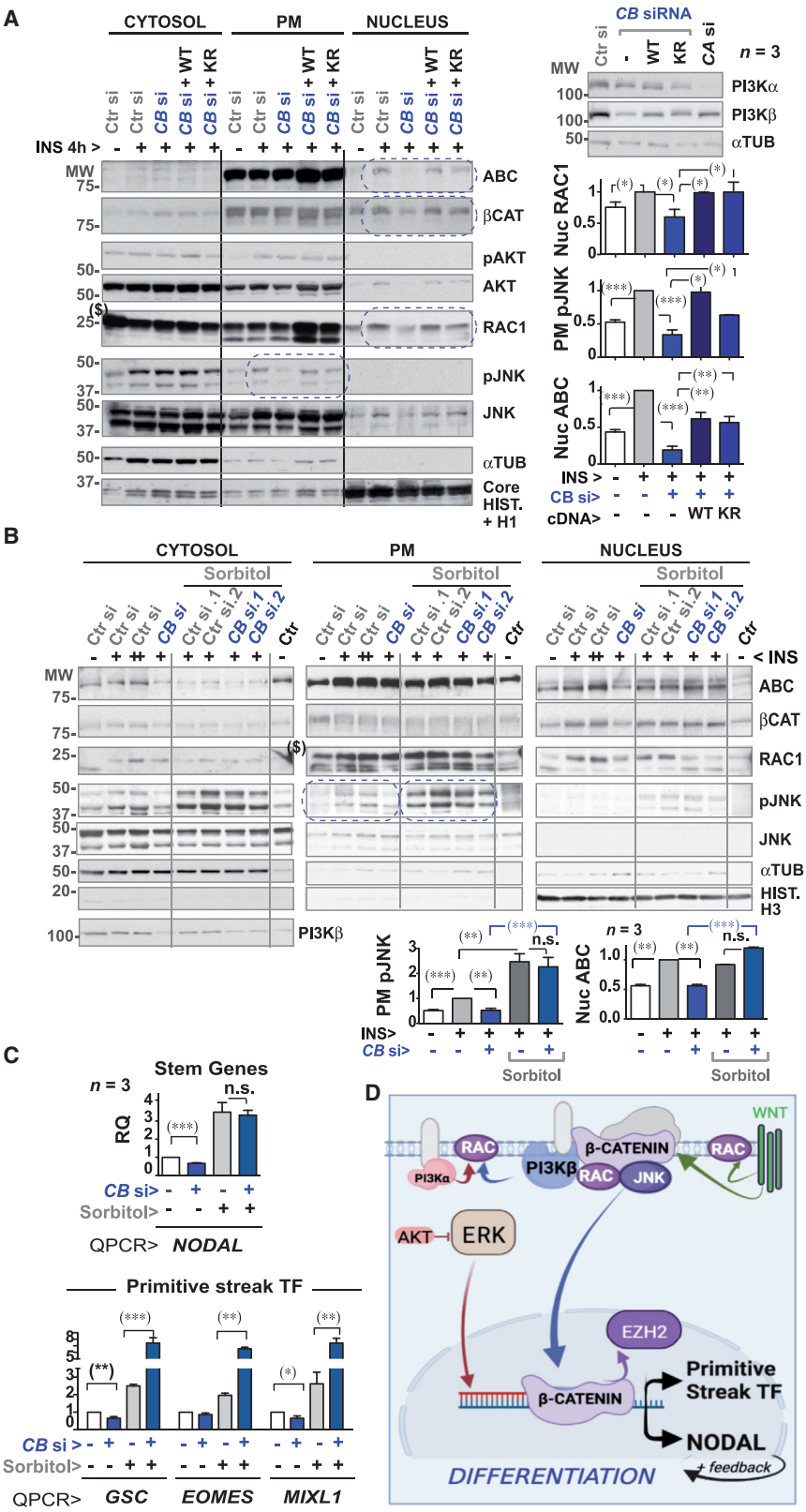

Figure 6. PI3Kβ controls Nuc RAC1, JNK activation, and β-Catenin Nuc content

(A) HEK293T cells were transfected with siRNA (72 h); 24 h later, some of the cells were transfected with WT or KR PI3Kβ cDNAs (48 h). Prior to collection, cells were incubated in medium without serum (90 min) and then treated with INS (10 μg/mL, 4 h). Extracts were examined by WB. Graphs show the signal in each condition corrected for the loading control and normalized to the signal in the INS-treated DMSO control, considered 1. A $ symbol in the RAC1 blot indicates that the signal corresponds to the 25-kDa MW marker (added in this lane).

(B) hESCs transfected with control or *PIK3CB* siRNA (72 h) were incubated with GF-free medium (16 h) and then activated with INS (10 μg/mL or 20 μg/mL in lane ++) (90 min); 0.2 M sorbitol was added to the indicated samples (last 60 min). Extracts were tested by WB. Graphs are as in (A).

(C) Control and PI3Kβ-depleted hESCs (72 h) growing in mTeSR1were treated with the JNK activator sorbitol (0.2 M) (40 min) and then changed to mTeSR1 without sorbitol (3.5 h). The graphs show the mRNA levels of different genes in control and PI3Kβ-depleted cells.

(A–C) Mean ± SD, n ≥ 3; *p < 0.05, **p < 0.01, ***p < 0.001 (t test). Ellipses indicate the most relevant data.

(D) The drawing illustrates the mechanism of PI3Kβ contribution to β-catenin deposition (and EZH2 displacement) at *NODAL* and PS TF promoters. Activation of GF receptors for bFGF or INS (gray ellipses) or for WNT (green) trigger RAC1 activation; the PI3Kβ scaffold function stabilizes active RAC1, which, in turn, induces JNK activation and β-catenin Nuc accumulation. At the nucleus, PI3Kβ-regulated β-catenin induces EZH release from *NODAL* and PS gene promoters. NODAL further enhances *NODAL* transcription by positive feedback.

to examine gene expression. Sorbitol rescued *NODAL* and PS TF levels in PI3Kβ-depleted cells (Figure 6C), supporting the theory that *NODAL*/*PS* TF expression requires PI3Kβ control of active RAC1/JNK levels and, in turn, of nuclear β-catenin (Figures 6D and S6B).

PI3Kβ expression increases at advanced stages in several cancer types (Wymann and Marone, 2005). Cancer stem cells normally appear in high-stage tumors. We tested whether PI3Kβ contributed to the stemness features in cancer stem cells. Two squamous cell lung cancer (LUSC) cell lines, H226 and HCC15, were incubated under hypoxia or cultured in Matrigel/mTeSR1 to improve expression of stem cell markers (Figure S6C). PI3Kβ depletion reduced SOX2, OCT4, and NANOG levels in NCI-HCC15 cells and tended to reduce them in the NCI-H226 cells (Figure S6D). Thus, PI3Kβ might regulate stemness features in cancer cells.

DISCUSSION

Identifying the signals that maintain stemness or initiate hESC differentiation is of interest for applied medicine. To learn about these processes, the consequences of interfering with PI3Kα or PI3Kβ in primed hESCs were examined. To initiate differentiation, it is essential to remove PRC repression from the promoters of differentiation genes, but little was known about how PRC release is triggered at the onset of differentiation. This study shows that β-catenin triggers EZH2/PRC2 removal from *NODAL* and from PS gene promoters and that PI3Kβ is essential for this process. The results also show that fine-tuned control of PI3K activity and PI3Kβ scaffolding (non-catalytic) actions is needed for the cells to remain pluripotent or differentiate. PI3K activity maintained stemness by repressing ERK, and the PI3Kβ scaffolding action contributed to stemness by controlling *NODAL* levels as exogenous NODAL addition rescued pluripotency in PI3Kβ-depleted cells. PI3Kβ expression also regulated PS TF expression. At the molecular level, PI3Kβ, which binds to active-RAC1 (Fritsch et al., 2013), controlled RAC1 capacity to activate JNK and, in turn, β-catenin. Accordingly, exogenous activation of JNK in PI3Kβ-depleted hESCs rescued nuclear β-catenin levels and *NODAL* and PS TF expression. Thus, although intact PI3Kα activity contributes to stemness by repressing ERK activity and precocious differentiation, PI3Kβ scaffolding action guarantees β-catenin-mediated expression of *NODAL*. PI3Kβ also triggered β-catenin deposition and EZH2 removal from PS TF promoters. At the onset of differentiation, when WNT levels increase, PI3K levels decrease, and ERK activation increases; PI3Kβ expression is required for WNT- and GF-induced RAC/JNK/β-catenin activation and, in turn, for *NODAL* and PS TF expression (scheme in Figure S6B).

PI3K activity and PI3Kβ scaffold actions make critical contributions to stemness. The PI3Kβ scaffolding requirement for stemness was unrelated to core stem cell genes (whose levels decreased later than those of *NODAL*) or to MYC (which regulated different genes than PI3Kβ). PI3Kβ depletion reduced *NODAL* levels (a gene essential for stemness) (James et al., 2005), and exogenous NODAL addition rescued stemness in *PIK3CB*-silenced hESCs. This indicated that PI3Kβ controls stemness at least in part by regulating *NODAL*. The reduction of stem cell markers after PI3Kβ depletion in two LUSC cell lines (Figure S6D) supports the idea that PI3Kβ might also contribute to maintain the cancer stem cell phenotype.

Apart from the PI3Kβ scaffold function, PI3K activity was required for stemness. Throughout the present study, the consequences of depleting PI3Kα (which has greater kinase activity than PI3Kβ) (Marqués et al., 2009) returned results with the same tendency as those obtained by inhibiting PI3K, supporting the notion that the more important action of PI3Kα is catalytic. PI3Kα contribution to stemness has been suggested previously in induced pluripotent stem cells (Madsen et al., 2019) and in hESCs treated with a pan-PI3K inhibitor or deprived of GF (Singh et al., 2012). In the latter study, the authors elegantly showed that PI3K activity restricts ERK activity, which is required for stemness. Short-term PI3K inhibitor treatment reduced PI3K/AKT activity and increased pERK, but prolonged PI3K inhibition (48 h) or depletion (72 h) failed to reduce pAKT levels but still increased pERK. pAKT upregulation upon long-term PI3K inhibition also occurs in cancer and is due to abrogation of the negative feedback pathways that control PI3K/AKT transient activation (Rozengurt et al., 2014). Thus, the unrestricted ERK activity is most likely responsible for triggering differentiation in PI3Kα-depleted or PI3K-inhibited (48 h) hESCs, supporting the theory that PI3K activity controls stemness by restraining ERK.

At the onset of differentiation, both PI3K isoform levels decrease, diminishing the brake imposed by PI3K on ERK, which promotes cell differentiation (Na et al., 2010). In addition, WNT secretion in the epiblast triggers a pathway that protects β-catenin from degradation and exerts positive feedback on ERK activity (MacDonald and He, 2012; Kim et al., 2007). Despite the decrease in PI3Kβ levels at this stage, PI3Kβ expression was still required for expression of the PS TF. Indeed, PI3Kβ upregulated the expression of six (*GATA 6*, *MIXL1*, *GSC*, *SOX17*, *EOMES*, and *T*; Figures 1C and S2B)] of the 10 TF reported to control PS formation (Yoney et al., 2018; Scialdone et al., 2016). The PI3Kβ requirement for PS TF expression was confirmed in exponentially growing hESCs, in GSK3-inhibited hESCs, and in EBs.

The most relevant conclusion of the presented data is a novel function of β-catenin, which, after deposition in

NODAL and the PS TF promoters, triggers PRC/EZH2 release. In line with this function, WNT-regulated promoters are bound to EZH2 (Collinson et al., 2016). The β-catenin/EZH2 exchange was demonstrated in intact hESCs (Figure 4A), showing that, beyond the PI3Kβ contribution, the β-catenin/EZH2 exchange is a general mechanism for polycomb repression release in hESCs. The association of β-catenin with K-demethylases and chromatin remodelers might help to mediate EZH2 removal, acting as a pioneer cofactor (Li et al., 2017; Balsalobre and Drouin, 2022).

In all the cases tested (exponential growth, INS- or BIO-treated cells), PI3Kβ expression was essential for nuclear localization of RAC1 and β-catenin in hESCs. The kinase activity of PI3Kβ seemed not to be required because expression of WT or kinase-dead PI3Kβ rescued nuclear RAC1/β-catenin levels equally well in PI3Kβ-depleted hESCs. In contrast, p-Ser552-β-catenin levels (AKT dependent), which modulate nuclear β-catenin levels, did not explain the action of PI3Kβ in hESCs. In agreement with the critical role of a non-catalytic PI3Kβ action on nuclear β-catenin, PI3K inhibition only partially reduces WNT-induced gene expression (Wu et al., 2008). Only active forms of RAC1 localize to the nucleus (Lanning et al., 2003), and PI3Kβ reduced nuclear RAC1 (Figures 5 and 6). As for RAP1, its activation stabilizes and enhances β-catenin nuclear levels (Griffin et al., 2018), but nuclear RAP1 levels were similarly reduced by PI3Kβ inhibition or depletion without explaining the selective action of PI3Kβ depletion.

The presented data show that a PI3Kβ scaffold action is essential for nuclear localization of active RAC1, to increase pJNK levels at the PM, and to trigger β-catenin nuclear accumulation (Figures 5A, 5B, 6A, and 6B). PI3Kβ-dependent β-catenin nuclear accumulation was also detected in cells treated with a GSK3 inhibitor that mimics the WNT pathway. In support of PI3Kβ involvement in active RAC1/JNK-mediated β-catenin nuclear localization, exogenous activation of JNK corrected β-catenin nuclear levels and gene expression defects of hESCs depleted of PI3Kβ (Figures 6A and 6B). Thus, regulation of the RAC1/JNK/nuclear β-catenin axis is at least part of the mechanism for PI3Kβ action in hESCs.

The exact level at which PI3Kβ controls active RAC1 remains to be studied. RAC1 activation requires PI3K activity (e.g., Han et al., 1998). However, V^{12}RAC expression levels (not those of WT RAC1) were markedly lower in PI3Kβ-depleted HEK293T cells (data not shown). It is possible that PI3Kβ binding to active RAC1 (Fritsch et al., 2013) increases active RAC1 stability and, in turn, RAC1 nuclear entry. As for the mechanism of active RAC1 control of nuclear β-catenin, there are different models (any in hESC). The RAC1 C-terminal polybasic region binds to armadillo domain-containing proteins (e.g., β-catenin) and triggers their nuclear localization (Lanning et al., 2003). Active RAC1 associates with β-catenin and TCF-4 to enter the nucleus and control gene expression (Esufali and Bapat, 2004). RAC1 activates JNK (Coso et al., 1995), which phosphorylates β-catenin at the PM, triggering its nuclear translocation (Wu et al., 2008); β-catenin translocation from the PM to the nucleus is also induced by WNT (Jamieson et al., 2015). GFs induce RAC1 and JNK activation at the PM (Han et al., 1998; Neisch et al., 2010) and promote PI3Kβ translocation to the PM and the nucleus (Figure S5D). It is thus possible that RAC1 "switching on" occurs in the membrane, where it activates JNK, which, in turn, phosphorylates β-catenin, triggering its translocation to the nucleus. This model is supported by observations of co-localization of PI3Kβ and RAC1 at the PM (Cizmecioglu et al., 2016). Although this model remains to be studied, it explains PI3Kβ modulation of active RAC1 nuclear levels and pJNK PM levels (Figure 6A).

PI3K activity and scaffolding actions cooperate in hESC stemness maintenance. After GF addition, PI3Kα activation restricts ERK activation (Singh et al., 2012), preventing precocious expression of differentiation genes, and PI3Kβ permits active RAC1/JNK-mediated β-catenin nuclear localization and *NODAL* expression (required for stemness). PI3K activity increases in response to environmental GF. PI3Kβ scaffolding actions are also unmasked in response to GF addition because PI3Kβ binding to RAC1 requires prior activation of RAC1 by GF. RAC1 induces PI3Kβ localization at the PM (Cizmecioglu et al., 2016), and PI3Kβ ensures RAC1-mediated JNK activation and subsequent β-catenin nuclear accumulation (Figures 5A, 5B, 6A, and 6B). At the onset of PS formation, PI3Kα and PI3Kβ levels (and global PI3K activity) decrease (Figure S4C), and new environmental cues (e.g., BMP4 upregulation in extra-embryonic ectoderm and secretion of WNT in the epiblast) help to stabilize β-catenin. Although PI3Kα and β levels decrease, PI3Kβ-dependent β-catenin activation is still required for EZH2 removal from promoters of *NODAL* and of the TFs that trigger PS formation.

These results reveal the involvement of β-catenin in release of EZH2 from *NODAL* and PS genes promoters, a previously unknown function of β-catenin. The different contribution of PI3K activity and PI3Kβ scaffolding on hESC gene expression in stemness and differentiation (scheme in Figure S6B and graphical abstract) is an example of the fine-tuned equilibrium that drives the stemness/differentiation decision. PI3Kβ scaffolding guarantees NODAL expression in stemness, and PI3K activity contributes to pluripotency by repressing ERK and, in turn, precocious differentiation gene expression. In contrast, at the onset of differentiation, PI3K level reduction releases ERK activation, permitting differentiation gene expression. At this stage, PI3Kβ scaffold action would still act via the active

RAC1/JNK/β-catenin pathway to trigger β-catenin/EZH2 exchange at the promoters of PS regulators. Knowledge of PI3K regulation of stemness might be useful for directing hESC differentiation.

EXPERIMENTAL PROCEDURES

Human cell culture and cDNAs

The hESCs used in this study are Shef-1 cells (Thomson et al., 1998) obtained from the Department of Biomedical Science, University of Sheffield (UK), and two derivatives of H1 hESCs: OCT4-EGFP and AI08e-PAX6YFP hESCs (Zwaka and Thomson, 2003; Yao et al., 2017) from the Wicell Institute (WI, USA). Approval to work with these lines was obtained from the Spanish National Embryo Ethical Committee (ISCIII). All hESCs were maintained on Matrigel-coated plates (Corning) using mTeSR1 or NODAL-free mTeSR7 medium (STEMCELL Technologies). H226 (CRL-5826) and HCC-15 (ACC-496) were obtained from the American Type Culture Collection and the DSMZ (Deutsche Sammlung von Mikroorganismen und Zellkulturen GmbH) collection. HEK293T cells were cultured as reported previously (Vallejo-Díaz et al., 2016). WT and KR PI3Kβ cDNAs have been described previously (Marqués et al., 2009).

Quantification and statistical analysis

Gene expression profiles were examined using Venny software (https://bioinfogp.cnb.csic.es/tools/venny/). We used MATLAB software for log ratio representations of gene expression and for Pearson correlations. GO group analysis was performed using Genecodis3 software (https://bio.tools/genecodis3). Heatmap analysis was undertaken using MeV software. GSEA was performed at https://www.gsea-msigdb.org. In the figures, n indicates the number of independent experiments performed for each assay; statistical analysis methods are described in the figure legends. The statistical analysis was carried out using two-tailed unpaired Student's t test, chi-square test, and Pearson correlation using Prism 6 software (GraphPad). Differences were considered significant when $p < 0.05$. Fiji/ImageJ software was used for signal quantitation.

Data availability

The gene expression experiments included in this manuscript are deposited in GEO (GSE202163). Original blots are deposited at Mendeley data: https://doi.org/10.17632/m9g4fcvrm8.1.

SUPPLEMENTAL INFORMATION

Supplemental information can be found online at https://doi.org/10.1016/j.stemcr.2022.09.003.

ACKNOWLEDGMENTS

We thank A. Burton for English editing, A. Millán for help with AP staining, M. Chagoyen for assistance with gene expression analysis, C. Martinez-A. and A. Futterer for support with EB, and V. Calvanese, M. Torres, and G. Giovinazzo for assistance with the initial stages of the study. This work was funded by the Spanish Ministry of Science, Innovation and Universities (SAF2016-79195-R and PID2019-106937RB-I00), by the Madrid Regional Government (S2017/BMD-3804), and by the Spanish Association Against Cancer (16035CARR). V.P.-G. was supported by the Spanish Ministry of Science and Innovation (RYC-2019-026956 and PID2020-114459RA-I00).

AUTHOR CONTRIBUTIONS

S.Y. performed most of the experiments. A.G. and M.C.H. helped with some experiments. V.P.-G., initiated the project. J.C.O. helped with datasets analysis. M.F.F. discussed experiments. A.C.C. directed the work, wrote the manuscript, and helped with some experiments.

CONFLICT OF INTERESTS

The authors declare no competing interests.

Received: May 24, 2022
Revised: September 1, 2022
Accepted: September 2, 2022
Published: September 29, 2022

REFERENCES

Aranda, S., Mas, G., and Di Croce, L. (2015). Regulation of gene transcription by Polycomb proteins. Sci. Adv. *1*, e1500737. https://doi.org/10.1126/sciadv.1500737.

Balsalobre, A., and Drouin, J. (2022). Pioneer factors as master regulators of the epigenome and cell fate. Nat. Rev. Mol. Cell Biol. *23*, 449–464. https://doi.org/10.1038/s41580-022-00464-z.

Bi, L., Okabe, I., Bernard, D.J., Wynshaw-Boris, A., and Nussbaum, R.L. (1999). Proliferative defect and embryonic lethality in mice homozygous for a deletion in the p110α subunit of PI3K. J. Biol. Chem. *274*, 10963–10968. https://doi.org/10.1074/jbc.274.16.10963.

Bi, L., Okabe, I., Bernard, D.J., and Nussbaum, R.L. (2002). Early embryonic lethality in mice deficient in the p110β catalytic subunit of PI3K. Mamm. Genome *13*, 169–172. https://doi.org/10.1007/BF02684023.

Beattie, G.M., López, A.D., Bucay, N., Hinton, A., Firpo, M.T., King, C.C., and Hayek, A. (2005). Activin A maintains pluripotency of human embryonic stem cells in the absence of feeder layers. Stem Cell. *23*, 489–495. https://doi.org/10.1634/stemcells.2004-0279.

Bertero, A., Madrigal, P., Galli, A., Hubner, N.C., Moreno, I., Burks, D., Brown, S., Pedersen, R.A., Gaffney, D., Mendjan, S., et al. (2015). Activin/nodal signaling and NANOG orchestrate human embryonic stem cell fate decisions by controlling the H3K4me3 chromatin mark. Genes Dev. *29*, 702–717. https://doi.org/10.1101/gad.255984.114.

Ciraolo, E., Iezzi, M., Marone, R., Marengo, S., Curcio, C., Costa, C., Azzolino, O., Gonella, C., Rubinetto, C., Wu, H., et al. (2008). Phosphoinositide 3-kinase p110beta activity: key role in metabolism and mammary gland cancer but not development. Sci. Signal. *1*, ra3. https://doi.org/10.1126/scisignal.1161577.

Cizmecioglu, O., Ni, J., Xie, S., Zhao, J.J., and Roberts, T.M. (2016). RAC1-mediated membrane raft localization of PI3K/p110β is required for its activation by GPCRs or PTEN loss. Elife *5*, e17635. https://doi.org/10.7554/eLife.17635.

Collinson, A., Collier, A.J., Morgan, N.P., Sienerth, A.R., Chandra, T., Andrews, S., and Rugg-Gunn, P.J. (2016). Deletion of the polycomb-group protein EZH2 leads to compromised self-renewal and differentiation defects in human embryonic stem cells. Cell Rep. *17*, 2700–2714. https://doi.org/10.1016/j.celrep.2016.11.032.

Coso, O.A., Chiariello, M., Yu, J.C., Teramoto, H., Crespo, P., Xu, N., Miki, T., and Gutkind, J.S. (1995). The small GTP-binding proteins Rac1 and Cdc42 regulate the activity of the JNK/SAPK signaling pathway. Cell *81*, 1137–1146. https://doi.org/10.1016/s0092-8674(05)80018-2.

Cross, D.A., Alessi, D.R., Cohen, P., Andjelkovich, M., and Hemmings, B.A. (1995). Inhibition of GSK-3 by insulin mediated by protein kinase B. Nature *378*, 785–789. https://doi.org/10.1038/378785a0.

Dakhore, S., Nayer, B., and Hasegawa, K. (2018). Human pluripotent stem cell culture: current status, challenges, and advancement. Stem Cell. Int. *2018*, 7396905. https://doi.org/10.1155/2018/7396905.

Ding, Q., Xia, W., Liu, J.-C., Yang, J.-Y., Lee, D.-F., Xia, J., Bartholomeusz, G., Li, Y., Pan, Y., Li, Z., et al. (2005). Erk associates with and primes GSK-3β for its inactivation resulting in upregulation of β-CATENIN. Mol. Cell *19*, 159–170. https://doi.org/10.1016/j.molcel.2005.06.009.

Esufali, S., and Bapat, B. (2004). Cross-talk between RAC1 GTPase and dysregulated Wnt signaling pathway leads to cellular redistribution of beta-CATENIN and TCF/LEF-mediated transcriptional activation. Oncogene *23*, 8260–8271. https://doi.org/10.1038/sj.onc.1208007.

Fang, D., Hawke, D., Zheng, Y., Xia, Y., Meisenhelder, J., Nika, H., Mills, G.B., Kobayashi, R., Hunter, T., and Lu, Z. (2007). Phosphorylation of β-catenin by AKT promotes β-catenin transcriptional activity. J. Biol. Chem. *282*, 11221–11229. https://doi.org/10.1074/jbc.M611871200.

Funa, N.S., Schachter, K.A., Lerdrup, M., Ekberg, J., Hess, K., Dietrich, N., Honoré, C., Hansen, K., and Semb, H. (2015). β-Catenin regulates primitive streak induction through collaborative interactions with SMAD2/SMAD3 and OCT4. Cell Stem Cell *16*, 639–652. https://doi.org/10.1016/j.stem.2015.03.008.

Fritsch, R., de Krijger, I., Fritsch, K., George, R., Reason, B., Kumar, M.S., Diefenbacher, M., Stamp, G., and Downward, J. (2013). RAS and RHO families of GTPases directly regulate distinct phosphoinositide 3-kinase isoforms. Cell *153*, 1050–1063. https://doi.org/10.1016/j.cell.2013.04.031.

Greber, B., Lehrach, H., and Adjaye, J. (2008). Control of early fate decisions in human ES cells by distinct states of TGFβ pathway activity. Stem Cell. Dev. *17*, 1065–1077. https://doi.org/10.1089/scd.2008.0035.

Griffin, J.N., Del Viso, F., Duncan, A.R., Robson, A., Hwang, W., Kulkarni, S., Liu, K.J., and Khokha, M.K. (2018). RAPGEF5 regulates nuclear translocation of β-catenin. Dev. Cell *44*, 248–260.e4. https://doi.org/10.1016/j.devcel.2017.12.001.

Han, J., Luby-Phelps, K., Das, B., Shu, X., Xia, Y., Mosteller, R.D., Krishna, U.M., Falck, J.R., White, M.A., and Broek, D. (1998). Role of substrates and products of PI 3-kinase in regulating activation of Rac-related guanosine triphosphatases by Vav. Science *279*, 558–560. https://doi.org/10.1126/science.279.5350.558.

Huggins, I.J., Bos, T., Gaylord, O., Jessen, C., Lonquich, B., Puranen, A., Richter, J., Rossdam, C., Brafman, D., Gaasterland, T., et al. (2017). The WNT target SP5 negatively regulates WNT transcriptional programs in human pluripotent stem cells. Nat. Commun. *8*, 1034. https://doi.org/10.1038/s41467-017-01203-1.

James, D., Levine, A.J., Besser, D., and Hemmati-Brivanlou, A. (2005). TGFβ/activin/nodal signaling is necessary for the maintenance of pluripotency in human embryonic stem cells. Development *132*, 1273–1282. https://doi.org/10.1242/dev.01706.

Jamieson, C., Lui, C., Brocardo, M.G., Martino-Echarri, E., and Henderson, B.R. (2015). Rac1 augments Wnt signaling by stimulating β-catenin-lymphoid enhancer factor-1 complex assembly independent of β-catenin nuclear import. J. Cell Sci. *128*, 3933–3946. https://doi.org/10.1242/jcs.167742.

Kim, D., Rath, O., Kolch, W., and Cho, K.H. (2007). A hidden oncogenic positive feedback loop caused by crosstalk between Wnt and ERK pathways. Oncogene *26*, 4571–4579. https://doi.org/10.1038/sj.onc.1210230.

Lanning, C.C., Ruiz-Velasco, R., and Williams, C.L. (2003). Novel mechanism of the co-regulation of nuclear transport of SmgGDS and Rac1. J. Biol. Chem. *278*, 12495–12506. https://doi.org/10.1074/jbc.M211286200.

Li, J., Yu, B., Deng, P., Cheng, Y., Yu, Y., Kevork, K., Ramadoss, S., Ding, X., Li, X., and Wang, C.Y. (2017). KDM3 epigenetically controls tumorigenic potentials of human colorectal cancer stem cells through Wnt/β-catenin signalling. Nat. Commun. *8*, 15146. https://doi.org/10.1038/ncomms15146.

Li, Y.Q. (2010). Master stem cell transcription factors & signaling regulation. Cell. Reprogram. *12*, 3–13. https://doi.org/10.1089/cell.2009.0033.

Na, J., Furue, M.K., and Andrews, P.W. (2010). Inhibition of ERK1/2 prevents neural and mesendodermal differentiation and promotes human embryonic stem cell self-renewal. Stem Cell Res. *5*, 157–169. https://doi.org/10.1016/j.scr.2010.06.002.

Neisch, A.L., Speck, O., Stronach, B., and Fehon, R.G. (2010). Rho1 regulates apoptosis via activation of the JNK signaling pathway at the plasma membrane. J. Cell Biol. *189*, 311–323. https://doi.org/10.1083/jcb.200912010.

Niwa, H. (2007). How is pluripotency determined and maintained? Development *134*, 635–646. https://doi.org/10.1242/dev.02787.

MacDonald, B.T., and He, X. (2012). Frizzled and LRP5/6 receptors for Wnt/β-CATENIN signaling. Cold Spring Harb. Perspect. Biol. *4*, a007880. https://doi.org/10.1242/dev.02787.

Madsen, R.R., Knox, R.G., Pearce, W., Lopez, S., Mahler-Araujo, B., McGranahan, N., Vanhaesebroeck, B., and Semple, R.K. (2019). Oncogenic PIK3CA promotes cellular stemness in an allele dose-dependent manner. Proc. Natl. Acad. Sci. USA *116*, 8380–8389. https://doi.org/10.1073/pnas.1821093116.

Mansergh, F.C., Daly, C.S., Hurley, A.L., Wride, M.A., Hunter, S.M., and Evans, M.J. (2009). Gene expression profiles during early differentiation of mouse embryonic stem cells. BMC Dev. Biol. *9*, 5. https://doi.org/10.1186/1471-213X-9-5.

Marqués, M., Kumar, A., Poveda, A.M., Zuluaga, S., Hernández, C., Jackson, S., Pasero, P., and Carrera, A.C. (2009). Specific function of PI 3-kinase beta in the control of DNA replication. Proc. Natl. Acad. Sci. USA *106*, 7525–7530. https://doi.org/10.1073/pnas.0812000106.

Mateus, A.M., Gorfinkiel, N., and Arias, A.M. (2009). Origin and function of fluctuations in cell behaviour and the emergence of patterns. Semin. Cell Dev. Biol. *20*, 877–884. https://doi.org/10.1016/j.semcdb.2009.07.009.

Olazábal-Morán, M., Sánchez-Ortega, M., Martínez-Muñoz, L., Hernández, C., Rodríguez, M.S., Mellado, M., and Carrera, A.C. (2021). Fluctuations in AKT and PTEN activity are linked by the E3 ubiquitin ligase cCBL. Cells *10*, 2803. https://doi.org/10.3390/cells10112803.

Rozengurt, E., Soares, H.P., and Sinnet-Smith, J. (2014). Suppression of feedback loops mediated by PI3K/mTOR induces multiple overactivation of compensatory pathways: an unintended consequence leading to drug resistance. Mol. Cancer Ther. *13*, 2477–2488. https://doi.org/10.1158/1535-7163.MCT-14-0330.

Sakaki-Yumoto, M., Liu, J., Ramalho-Santos, M., Yoshida, N., and Derynck, R. (2013). Smad2 is essential for maintenance of the human and mouse primed pluripotent stem cell state. J. Biol. Chem. *288*, 18546–18560. https://doi.org/10.1074/jbc.M112.446591.

Singh, A.M., Reynolds, D., Cliff, T., Ohtsuka, S., Mattheyses, A.L., Sun, Y., Menéndez, L., Kulik, M., and Dalton, S. (2012). Signaling network crosstalk in human pluripotent cells: a Smad2/3-regulated switch that controls the balance between self-renewal and differentiation. Cell Stem Cell *10*, 312–326. https://doi.org/10.1016/j.stem.2012.01.014.

Scialdone, A., Tanaka, Y., Jawaid, W., Moignard, V., Wilson, N.K., Macaulay, I.C., Marioni, J.C., and Göttgens, B. (2016). Resolving early mesoderm diversification through single-cell expression profiling. Nature *535*, 289–293. https://doi.org/10.1038/nature18633.

Skottman, H., Mikkola, M., Lundin, K., Olsson, C., Strömberg, A.M., Tuuri, T., Otonkoski, T., Hovatta, O., and Lahesmaa, R. (2005). Gene expression signatures of seven individual human embryonic stem cell lines. Stem Cell. *23*, 1343–1356. https://doi.org/10.1634/stemcells.2004-0341.

Storm, M.P., Bone, H.K., Beck, C.G., Bourillot, P.-Y., Schreiber, V., Damiano, T., Nelson, A., Savatier, P., and Welham, M.J. (2007). Regulation of Nanog expression by PI3K-dependent signaling in murine embryonic stem cells. J. Biol. Chem. *282*, 6265–6273. https://doi.org/10.1074/jbc.M610906200.

Takahashi, K., and Yamanaka, S. (2006). Induction of pluripotent stem cells from mouse embryonic and adult fibroblast cultures by defined factors. Cell *126*, 663–676. https://doi.org/10.1016/j.cell.2006.07.024.

Thomson, J.A., Itskovitz-Eldor, J., Shapiro, S.S., Waknitz, M.A., Swiergiel, J.J., Marshall, V.S., and Jones, J.M. (1998). Embryonic stem cell lines derived from human blastocysts. Science *282*, 1145–1147. https://doi.org/10.1126/science.282.5391.1145.

Vallejo-Díaz, J., Olazabal-Morán, M., Cariaga-Martínez, A.E., Pajares, M.J., Flores, J.M., Pio, R., Montuenga, L.M., and Carrera, A.C. (2016). Targeted depletion of PIK3R2 induces regression of lung squamous cell carcinoma. Oncotarget *7*, 85063–85078. https://doi.org/10.18632/oncotarget.13195.

Wang, J., Sinha, T., and Wynshaw-Boris, A. (2012). Wnt signaling in mammalian development: lessons from mouse genetics. Cold Spring Harb. Perspect. Biol. *4*, a007963. https://doi.org/10.1101/cshperspect.a007963.

Wymann, M.P., and Marone, R. (2005). Phosphoinositide 3-kinase in disease: timing, location, and scaffolding. Curr. Opin. Cell Biol. *17*, 141–149. https://doi.org/10.1016/j.ceb.2005.02.011.

Wu, X., Tu, X., Joeng, K.S., Hilton, M.J., Williams, D.A., and Long, F. (2008). RAC1 activation controls nuclear localization of beta-CATENIN during canonical Wnt signaling. Cell *133*, 340–353. https://doi.org/10.1016/j.cell.2008.01.052.

Yao, Z., Mich, J.K., Ku, S., Menon, V., Krostag, A.-R., Martínez, R.A., Furchtgott, L., Mulholland, H., Bort, S., Fuqua, M.A., et al. (2017). A single-cell roadmap of lineage bifurcation in human ESC models of embryonic brain development. Cell Stem Cell *20*, 120–134. https://doi.org/10.1016/j.stem.2016.09.011.

Yoney, A., Etoc, F., Ruzo, A., Carroll, T., Metzger, J.J., Martyn, I., Li, S., Kirst, C., Siggia, E.D., and Brivanlou, A.H. (2018). WNT signaling memory is required for ACTIVIN to function as a morphogen in human gastruloids. Elife *7*, e38279. https://doi.org/10.7554/eLife.38279.

Yu, P., Pan, G., Yu, J., and Thomson, J.A. (2011). FGF2 sustains NANOG and switches the outcome of BMP4-induced human embryonic stem cell differentiation. Cell Stem Cell *8*, 326–334. https://doi.org/10.1016/j.stem.2011.01.001.

Zheng, X., Dumitru, R., Lackford, B.L., Freudenberg, J.M., Singh, A.P., Archer, T.K., Jothi, R., and Hu, G. (2012). Cnot1, Cnot2, and Cnot3 maintain mouse and human ESC identity and inhibit extraembryonic differentiation. Stem Cell. *30*, 910–922. https://doi.org/10.1002/stem.1070.

Zwaka, T.P., and Thomson, J.A. (2003). Homologous recombination in human embryonic stem cells. Nat. Biotechnol. *21*, 319–321. https://doi.org/10.1038/nbt788.